Contribution from the Department of Chemistry,
University of Cincinnati, Cincinnati, Ohio 45221-0172

Structure of Trichloro(diethylenetriamine)gold(III), Au(dien)Cl_3, Determined by Single-Crystal X-ray Diffraction, Raman, and EXAFS Spectroscopies: An EXAFS Caveat

R. C. Elder* and J. W. Watkins II

Received June 14, 1985

EXAFS spectroscopy of solid samples suggests that Au(dien)Cl_3 is a molecular entity with pseudooctahedral coordination. The three nitrogen donors from the dien ligand and one chlorine form an equatorial plane with two axial Au–Cl bonds of uncertain length (2.6 or 3.0 Å) completing the coordination sphere. A single-crystal X-ray diffraction study confirms the overall structure but yields axial Au–Cl lengths of 3.121 (4) and 3.183 (3) Å. The crystals are orthorhombic, space group *Pbca*, with cell constants a = 12.442 (5), b = 12.878 (9), and c = 13.177 (3) Å and eight molecules per unit cell. These molecules were further characterized by Raman spectroscopy in solution as well as the solid state. Equatorial and axial Au–Cl stretching vibrations are observed for both phases, indicating some stability of the Au–Cl(axial) bonds in solution.

Introduction

Recently, we have determined the structures of gold-containing antiarthritis drugs and related gold-containing compounds, using both X-ray absorption spectroscopy and single-crystal X-ray diffraction.[1-4] Our principal interest has been to investigate the structural changes that take place in the vicinity of the gold atom when binding in a biological matrix occurs. Because the gold concentration in the biological samples is relatively low and the samples are noncrystalline, we have found that extended X-ray absorption fine structure (EXAFS) spectroscopy is a technique ideally suited to provide the structural information concerning the neighbors of the X-ray absorbing gold atom. We investigated the title compound, trichloro(diethylenetriamine)gold(III), Au(dien)Cl_3, as part of a study of the binding of gold complexes to albumin.[5] The EXAFS analysis suggested the possibility of an octahedral gold(III) complex with an equatorial plane formed by three nitrogen donors and one chlorine donor as well as two axial chlorine ligands at quite short Au–Cl distances. To check this possibility, we determined the single-crystal structure of this complex and report the EXAFS and diffraction results here, as well as the further characterization of this molecule by Raman spectroscopy.

Experimental Section

EXAFS Data Collection. A powdered, yellow sample of Au(dien)Cl_3 was obtained from Dr. C. Frank Shaw III, University of Wisconsin—Milwaukee. The sample was prepared for EXAFS analysis by mixing 8 mg of the gold complex with 31 mg of powdered $LiCO_3$ as the diluent. The amount of gold in the sample was chosen so that the value of $(\Delta\mu)x$, the change in the absorption coefficient times the thickness of the sample, was less than 1.0 to avoid a bias in the subsequent determination of coordination numbers (the "thickness effect").[6] The X-ray absorption spectra were collected at the Stanford Synchrotron Radiation Laboratory as previously described.[7] A Si(220), double-crystal monochromator and standard nitrogen-filled ionization chambers were used for the transmission-mode measurements. Wavelength calibration was obtained by the simultaneous measurement of gold-foil spectra. The energy range for data collection spanned 11.5–13.0 keV, encompassing the Au L_{III} absorption edge. A total of 220 data points were collected beyond the edge at evenly spaced intervals in k space with integration times varying from 1 to 12 s/point, the longer times being used for the points farther from the edge. Three scans were collected on the solid sample at room temperature and then averaged together.

EXAFS Data Analysis. The EXAFS data were extracted from the transmission measurements, $\log (I_0/I)$, by using the methods developed by Hodgson and co-workers.[8,9] The computer programs we use are local modifications of the programs originating with Hodgson's group.[10,11] The EXAFS spectrum was obtained by a background removal and the subtraction of a three-segment cubic spline. Plotting the extracted EXAFS data, times $\mathbf{k}^3$, where $\mathbf{k}$ is the photoelectron wave vector, results in the weighted EXAFS spectrum. The extracted EXAFS data were then Fourier transformed from frequency ($Å^{-1}$) space into radial distance (Å) space. This generates a radial-distribution-like function with peaks corresponding to absorber–scatterer pairs (Au–N, Au–Cl). The frequency component of the EXAFS data, corresponding to the desired absorber–scatterer pair(s), was obtained by back-transforming the region of the Fourier transform that is of interest. The back-transform utilized a square-window function for the Fourier filtering applied over the desired R range of the Fourier transform.

Structural parameters were extracted from the filtered EXAFS data by using empirical curve-fitting techniques. Model compounds containing a single type of scatterer in the first coordination sphere, with a known bond length and coordination number, were used to obtain the phase and amplitude functions of the absorber–scatterer pair (corresponding to $C(j,2)$, $C(j,3)$, $C(j,4)$, and $C(j,6)$ in eq 1). The filtered EXAFS data

$$\chi = \sum_{j=1}^{n} \frac{C(j,1)e^{-C(j,2)\mathbf{k}^2}}{\mathbf{k}^{C(j,3)}} \sin [C(j,4) + C(j,5)\mathbf{k} + C(j,6)\mathbf{k}^2] \quad (1)$$

of the gold–dien complex were then fit to the parametrized equation. The bond length and coordination number was determined by allowing $C(j,1)$ and $C(j,5)$ to vary in a nonlinear least-squares curve-fitting process. The absorber–scatterer distance was then calculated by $R_{unk} = R_{model} + [C(j,5)_{unk} - C(j,5)_{model}]/2$ and the number of back-scattering atoms as $N_{unk} = N_{model}[C(j,1)_{unk}R_{unk}^2]/[C(j,1)_{model}R_{model}^2]$. The following model compounds were used in this EXAFS analysis: $[P(C_6H_5)_4](AuCl_4)$, with a crystallographically determined Au–Cl bond length of 2.285 Å for the Au–Cl absorber–scatterer pair;[12] $[Au(NH_3)_4][(NO_3)_3]$, with a crystallographically determined Au–N bond length of 2.02 Å for the Au–N absorber–scatterer pair.[13]

X-ray Diffractometry Characterization. Crystals suitable for X-ray analysis were grown by a slow-diffusion technique using an aqueous solution of the complex with an overlayer of ethanol. Crystals were grown from the same powdered sample batch that was used for the EXAFS analysis. A yellow, polyhedral crystal of approximate dimensions 0.23 × 0.23 × 0.10 mm was mounted on a glass fiber. Cu Kα radiation was used with a precession camera to obtain the $hk0$, $hk1$, $0kl$, and $1kl$ layer photographs. The systematic absences of $hk0$ (h = odd), $h0l$ (l = odd), and $0kl$ (k = odd) indicate the orthorhombic space group *Pbca*.

A least-squares analysis of 15 intense reflections measured at 2θ values in the region $2\theta > 15°$ yielded cell constants of a = 12.442 (5) Å, b =

(1) Shaw, C. F., III; Schaeffer, N. A.; Elder, R. C.; Eidsness, M. K.; Trooster, J. M.; Calis, G. H. M. *J. Am. Chem. Soc.* **1984**, *106*, 3511.
(2) Elder, R. C.; Eidsness, M. K.; Heeg, M. J.; Tepperman, K. G.; Shaw, C. F., III; Schaeffer, N. A. *ACS Symp. Ser.* **1983**, *No. 209*, 385.
(3) Eidsness, M. K.; Elder, R. C. In "EXAFS and Near Edge Structure"; Hodgson, K. O., Hedman, B., Penner-Hahn, J. E., Eds.; Springer: Berlin, 1984; Vol. 3, p 83.
(4) Elder, R. C.; Zeiher, E. H. K.; Onady, M.; Whittle, R. R. *J. Chem. Soc., Chem. Commun.* **1981**, 900.
(5) Carlock, M. T.; Shaw, C. F., III; Eidsness, M. K.; Watkins, J. W., II; Elder, R. C. *Inorg. Chem.*, in press.
(6) Stern, E. A.; Kim, K. *Phys. Rev. B: Condens. Matter* **1981**, *23*, 3781.
(7) Vanderheyden, J. L.; Ketring, A. R.; Libson, K.; Heeg, M. J.; Roecher, L.; Motz, P.; Whittle, R.; Elder, R. C.; Deutsch, E. *Inorg. Chem.* **1984**, *23*, 3184.
(8) Cramer, S. P.; Hodgson, K. O. *Prog. Inorg. Chem.* **1979**, *25*, 1.
(9) Cramer, S. P.; Hodgson, K. O.; Stiefel, E. I.; Newton, W. E. *J. Am. Chem. Soc.* **1978**, *100*, 2748.
(10) Eccles, T. K. Ph.D. Thesis, Stanford University, 1977.
(11) Cramer, S. P. Ph.D. Thesis, Stanford University, 1977.
(12) Elder, R. C.; Ragle, H.; Eidsness, M. K.; Watkins, J. W., II, manuscript in preparation.
(13) Weishaupt, M.; Strahle, J. *Z. Naturforsch. B: Anorg. Chem., Org. Chem.* **1976**, *31B*, 554.

0020-1669/86/1325-0223$01.50/0

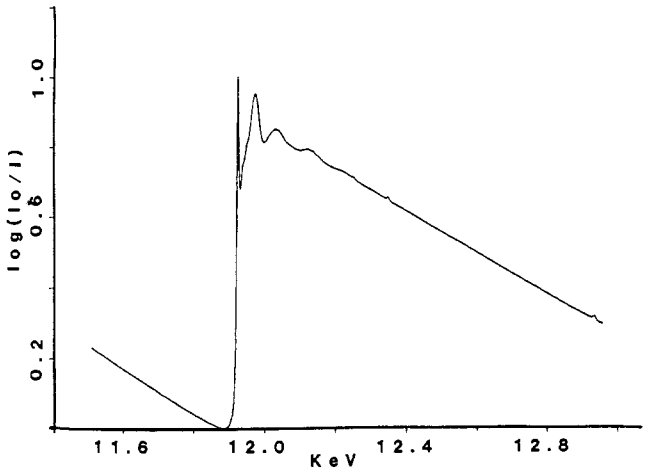

Figure 1. X-ray absorption spectrum for Au(dien)Cl_3. The intense, narrow peak occurring at ca. 11 920 eV is indicative of the +3 oxidation state of gold.

12.878 (9) Å, c = 13.177 (3) Å, and V = 2111.33 Å^3. For Z = 8 the calculated density is 2.56 g cm^{-3}, whereas the experimentally measured density is 2.57 (3) g cm^{-3} (as determined by neutral buoyancy in a mixture of 1,1,2,2-tetrabromoethane and carbon tetrachloride). Intensities were measured, by using our established procedure,[14] for 2859 reflections of the type $h,k,\pm l$ in the region $2.5 < 2\theta < 42°$. From these, 997 independent, observed reflections ($I > 3\sigma(I)$) were obtained by averaging. To monitor crystal stability and long-term drift, four standard reflections were measured after every 36 reflections. The drift correction varied randomly from 0.99 to 1.07. Empirical absorption corrections were applied[15] with the resulting intensity corrections varying from 1.07 to 2.09. The other details of data collection are as follows: scan method $2\theta/\theta$; scan rate 1–8°/min; scan range from 0.7° below the $K\alpha_1$ peak to 0.7° above the $K\alpha_2$ peak in 2θ; max h = 12, max k = 12, extreme l = ±13.

Structure Solution and Refinement. Zerovalent scattering curves from Cromer[16] were used for Au, Cl, N, and C. Scattering curves for hydrogen were taken from Stewart.[17] A Patterson vector map was calculated from the reduced diffraction data. From this map the positions of the gold and the equatorial chlorine atoms were determined. The remaining atom positions were determined by using difference Fourier techniques. All hydrogen atoms were placed at ideal positions and assigned an arbitrary isotropic temperature parameter, B, of 4.0 Å^2.[18] Refinement, based on F, of the positional parameters and the anisotropic thermal parameters of the non-hydrogen atoms led to a final convergence at R_1 = 0.031 and R_w = 0.036. A final difference Fourier map indicates eight unassigned peaks that are greater than 0.5 e Å^{-3}. The highest peak, representing approximately 1.0 e Å^{-3}, is located near one of the axial chlorine atoms, Cl(3). The remaining seven peaks, each representing 0.5–0.6 e Å^{-3}, are located, principally, around Cl(3) and the other axial chlorine atom, Cl(2). The location of these peaks suggests that the residual electron density stems from inadequate modeling of the thermal/vibrational disorder by the thermal ellipsoids. The values of the structure factors F_o and F_c are listed in Table A of the supplementary material.

Raman Spectroscopy. Spectra for solids and aqueous solutions were measured by using a Spex Ramalog spectrometer with a Coherent Innova 90 argon ion laser. The 514-nm emission was used for excitation with power levels of 0.5 W for solid-state and 1.0 W for solution measurements.

Results

EXAFS. The X-ray absorption near-edge structure (XANES) region of the spectrum was used to verify the oxidation state of the absorbing gold atoms. The edge inflection point energy is 11 920.1 eV, a value associated with the +3 oxidation state of gold.

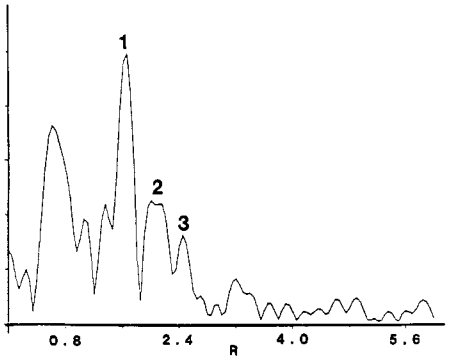

Figure 2. Fourier transform of the extracted EXAFS data. Peaks 1, 2, and 3 are attributable to Au–N and Au–Cl absorber–scatterer pairs.

Table I. EXAFS Results[a]

model	peak no.	calcd bond length, Å	calcd coord no.	fit
		Single-Shell Fits		
N	1	2.04	2.9	0.41
Cl	2	2.30	0.5	0.47
Cl(2.7)[a]	3	2.68	0.3	0.28
Cl(3.1)	3	2.99	0.4	0.27
		Two-Shell Fits		
N	1, 2	2.03	3.1	0.43
Cl		2.30	0.8	
Cl	2, 3	2.30	0.4	0.43
Cl(2.7)		2.61	0.5	
		Three-Shell Fits		
N	1, 2, 3	2.03	3.0	0.50
Cl		2.30	0.7	
Cl(2.7)		2.61	0.4	
N	1, 2, 3	2.03	3.1	0.49
Cl		2.30	0.8	
Cl(3.0)		2.99	0.5	

[a] The numbers in parentheses indicate the Au–Cl bond length that was used to determine the starting value of the bond length parameter.

Also indicative of the +3 oxidation state is the very intense peak in the XANES region (Figure 1). This peak is attributed to the 2p to 5d electronic transition that can occur for the Au(III) d^8 species but not for the Au(0) or Au(I) species, which have no 5d vacancy.[2]

Figure 2 is the Fourier transform of the EXAFS data from **k** = 3 to 16 Å^{-1}. Peaks 1, 2, and 3 are attributable to absorber–scatterer pairs of the type Au–X, where X is nitrogen or chlorine. The peaks occurring at R values lower than that of peak 1 regularly appear in EXAFS Fourier transforms and are at too short a distance to be attributable to absorber–scatterer pairs. Peak 1, occurring at 1.64 Å, arises from the three equatorial nitrogen atoms, peak 2, at 2.06 Å, is from the equatorial chlorine atom, and peak 3, at 2.42 Å, is from the two axial chlorine atoms. These peaks were back-transformed through the Fourier filter and used for empirical curve-fitting analysis as summarized in Table I.

A combination of single-shell and multishell curve-fitting analyses was used to determine the coordination environment of the gold atom. In the case of a single-shell analysis, where only one absorber–scatterer pair was investigated, the data of one peak in the Fourier transform were back-transformed through the Fourier filter for curve fitting with the model parameters of the absorber–scatterer pair; data from peak 1 were fit with parameters for an Au–N absorber–scatterer pair, and data from peaks 2 and 3 were fit with parameters for an Au–Cl absorber–scatterer pair. In the case of a multishell fit, two or three peaks from the Fourier transform were back-transformed together for curve fitting with parameters from the respective absorber–scatterer pairs. For example, peaks 1 and 2 were back-transformed together for curve fitting using the combination of Au–N and Au–Cl parameters. The results in Table I are grouped as to the number of shells that

(14) Elder, R. C.; Florian, L. R.; Lake, R. E.; Yacynych, A. M. *Inorg. Chem.* **1973**, *12*, 2690.
(15) Crenshaw, M. D.; Schmolka, S. J.; Zimmer, H.; Whittle, R.; Elder, R. C. *J. Org. Chem.* **1982**, *47*, 101.
(16) Cromer, D. T.; Mann, J. B. *Acta Crystallogr., Sect. A: Cryst. Phys., Diffr., Theor. Gen. Crystallogr.* **1968**, *A24*, 321.
(17) Stewart, R. F.; Davidson, E. R.; Simpson, W. T. *J. Chem. Phys.* **1965**, *42*, 3175.
(18) Isotropic thermal parameters are of the form $\exp(-B(\sin^2\theta/\lambda^2))$.

Table II. Atomic Positional Parameters for Non-Hydrogen Atoms of $Au(dien)Cl_3$[a,b]

atom	x	y	z
Au	0.27470 (3)	0.38986 (3)	0.40495 (3)
Cl(1)	0.1052 (2)	0.4448 (2)	0.4424 (2)
Cl(2)	0.2057 (2)	0.2141 (2)	0.2481 (2)
Cl(3)	0.3568 (2)	0.5576 (3)	0.5573 (3)
N(1)	0.2899 (6)	0.4775 (6)	0.2761 (6)
N(2)	0.4265 (6)	0.3462 (6)	0.3750 (6)
N(3)	0.2816 (7)	0.2784 (6)	0.5160 (6)
C(1)	0.4055 (8)	0.4699 (9)	0.2440 (8)
C(2)	0.4460 (8)	0.3616 (8)	0.2657 (8)
C(3)	0.4388 (9)	0.2379 (8)	0.4121 (8)
C(4)	0.3942 (8)	0.2379 (8)	0.5196 (8)

[a] The estimated error in the last digit is given in parentheses. This form is used throughout. [b] The numbering scheme is shown in Figure 3.

Table III. Bond Lengths (Å) and Angles (deg) for $Au(dien)Cl_3$

Au–Cl(1)	2.278 (3)	Au–N(1)	2.048 (8)
Au–Cl(2)	3.183 (3)	Au–N(2)	2.010 (8)
Au–Cl(3)	3.121 (4)	Au–N(3)	2.051 (8)
N(1)–C(1)	1.503 (13)	C(4)–N(3)	1.496 (13)
C(1)–C(2)	1.511 (15)	C(3)–C(4)	1.521 (15)
C(2)–N(2)	1.473 (13)	N(2)–C(3)	1.486 (13)
Cl(1)–Au–N(1)	95.38 (22)	Cl(3)–Au–N(2)	90.71 (23)
Cl(1)–Au–N(2)	177.75 (50)	Cl(3)–Au–N(3)	90.69 (24)
Cl(1)–Au–N(3)	95.82 (25)	N(1)–Au–N(2)	84.52 (31)
Cl(1)–Au–Cl(2)	96.40 (10)	N(1)–Au–N(3)	166.72 (29)
Cl(1)–Au–Cl(3)	87.08 (10)	N(2)–Au–N(3)	84.57 (32)
Cl(2)–Au–N(1)	83.00 (24)	Au–N(1)–C(1)	106.62 (60)
Cl(2)–Au–N(2)	85.81 (23)	C(2)–N(2)–C(3)	115.53 (76)
Cl(2)–Au–N(3)	88.68 (24)	C(4)–N(3)–Au	107.80 (59)
Cl(2)–Au–Cl(3)	176.51 (27)	N(1)–C(1)–C(2)	109.04 (84)
Cl(3)–Au–N(1)	96.99 (23)	C(3)–C(4)–N(3)	108.14 (80)

were used in the fit. The data corresponding to peaks 1 and 2 lead to convergence at virtually the same values for bond lengths and coordination numbers throughout these analyses. The data from peak 3, however, converge at two different minima depending on the starting value of the parameter that corresponds to the bond length.

Crystal Structure. The final fractional atomic positional parameters for the non-hydrogen atoms and their estimated standard deviations are listed in Table II. A list of bond lengths and angles can be found in Table III. The atomic positional parameters for the hydrogen atoms are listed in Table B, the anisotropic thermal parameters are listed in Table C, and the derived root-mean-square displacements are in Table D of the supplementary material. The ORTEP drawing, with the hydrogen atoms omitted for clarity, is shown in Figure 3. The complex is a pseudooctahedral structure. The nitrogens of the diethylenetriamine ligand occupy three of the equatorial coordination sites around the gold. The fourth equatorial site is occupied by a chlorine atom. The two axial sites are occupied by chlorine atoms at an elongated Au–Cl distance of ca. 3.15 Å.

Raman Spectra. These were measured for a solid sample of $[Au(dien)Cl_3]$, giving strong bands shifted by 258 and 368 cm^{-1} from the exciting line. An aqueous solution sample of this compound gave strong bands at 255 and 374 cm^{-1}. A solution spectrum taken 6 h after the material had dissolved was essentially identical.

Discussion

The EXAFS Fourier transform suggests an unusual but not unexpected[19] structure for the title compound, that is a pseudo-octahedral one with three short Au–N bonds, one short Au–Cl bond (completing the equatorial plane), and two longer Au–Cl bonds in the axial direction. As reviewed by Jones,[19] gold(III) structures are principally found to be square planar. Five- and six-coordinate cases are known, however, especially with nitrogen donors and chelating ligands. The most similar case is that of $Au(dien)Cl_2ClO_4$, for which an incompletely refined structure has been published[20] ($R = 0.12$). There the axial donors are Cl^- at 3.05 Å and an oxygen atom of the perchlorate ion a 3.10 Å.

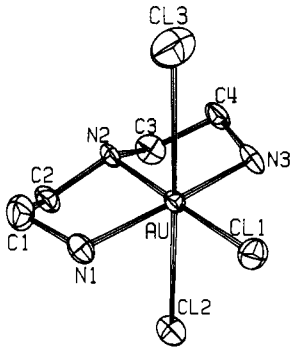

Figure 3. ORTEP diagram of $Au(dien)Cl_3$.

The EXAFS curve-fitting results are ambiguous about the Au–Cl(axial) bond lengths. Depending on the choice of the Au–Cl length with which the nonlinear least-squares process is started, different results are obtained. If we use the 2.4-Å position of peak 3 in the FT (Figure 2) and add an approximate phase shift of 0.3 Å, a starting value of 2.7 Å is generated and the calculation refines to a value of ca. 2.6 Å. If, on the other hand, we take a starting value of 3.1 Å in accord with the $Au(dien)Cl_2ClO_4$ crystal structure,[20] the calculation converges to 3.0 Å. The goodness of fit[21] indicates that we are unable to discriminate between the two results. Previous calculations from this laboratory,[22] fitting gold complexes of known crystal structure, have shown that choosing starting values differing by as little as 0.4 Å may result in convergence at different answers. However, in the gold–sulfur cases examined previously, convergence at the "wrong" value gave a significantly worse value for the goodness of fit (1.6 compared to 0.3, for example) in a single-shell case. Notice that here, whether the back-transform of peak 3 is treated as a single-shell fit or the back-transform of peaks 1, 2, and 3 as a three-shell fit, the resultant axial Au–Cl distance depends on the starting bond length. These ambiguities do not occur for the equatorial chlorine or nitrogen atoms with "normal" bond lengths but only occur for the significantly longer axial Au–Cl distance.

A final comment on the EXAFS calculation involves the coordination number of 0.5 that was determined for the equatorial chlorine atom in the single-shell fit. This error, representing a 50% deviation from the expected value of 1.0, probably stems from an inability to completely isolate and back-transform the frequency component associated with the Au–Cl(equatorial) pair from the neighboring peaks. When a two-shell or three-shell fit is performed, where the neighboring peak 1 is included in the back-transform, there is an increase in the Au–Cl(equatorial) coordination number while the bond length result remains virtually unchanged. The larger R range used in the back-transform eliminates a great deal of the effect of "lost amplitude" that results from trying to isolate a single peak from adjacent peaks; thus the calculated coordination number increases.

The possibility that the axial Au–Cl lengths might be as short as 2.6 Å led us to the single-crystal diffraction study. The structure refined easily to a relatively low value of the residual (0.031) and agrees with the general features expected from both the analogous chloro–perchlorato compound and the EXAFS analysis. However, there are differences in detail. For the two crystal structures, the equatorial Au–Cl distances agree: 2.278 (3) Å determined here

(19) Jones, P. G. *Gold Bull.* **1981**, *14*, 103, 159; **1983**, *16*, 114.

(20) Nardin, G.; Randaccio, L.; Annibale, G.; Natile, G.; Pitteri, B. *J. Chem. Soc., Dalton Trans.* **1980**, 220.

(21) Goodness of fit = $[\sum k^6(\text{data} - \chi)^2/N]^{1/2}$, where N is the number of data points. The lowest value of the function is assumed to give the parameters that best represent the structure. In general, values are only comparable for models using similar curve-fitting k ranges and the same number of shells.

(22) Eidsness, M. K. Ph.D. Thesis, University of Cincinnati, 1984.

Table IV

	EXAFS		crystal structure	
atoms	*R*, Å	CN	*R*, Å	CN
Au–N	2.03	3.1	2.04	3.0
$Au–Cl_{eq}$	2.30	0.8	2.28	1.0
$Au–Cl_{ax}$	2.61	0.5	3.15	2.0
	2.99	0.5		

as compared to 2.273 (8) Å found previously. The agreement in the Au–N bond lengths is poorer. For primary nitrogen donors, the values of 2.048 (8) and 2.051 (8) Å determined here should be compared to 1.97 (2) and 1.98 (2) Å found previously. For the secondary nitrogen donor of the dien ligand, the trends reverse: namely, in this structure Au–N(secondary) = 2.010 (8) Å, which is ca. 0.04 Å shorter than the Au–N(primary) distance. In the previous chloro–perchlorato structure, the secondary distance, 2.05 (2) Å, is ca. 0.06 Å longer than the primary distance. We know of no reason to suggest that such a reversal, if real, should occur other than, in general, Au–N distances have been shown[19] to be very variable. When it comes to the axial chlorine ligands, the biggest differences arise. The two distances determined here, 3.183 (3) and 3.121 (4) Å, differ by a large amount and differ even more from the value of 3.05 Å found previously for the Au–Cl(axial) distance. Although the average Au–Cl(axial) distance of 3.15 Å is rather long, it is significantly less than the 4.0-Å sum of the van der Waals radii (1.80 Å for Cl[23] and 2.2 Å for Au[24]). Also, the Au–Cl(2) and Au–Cl(3) vectors are nearly normal to the Au, Cl(1), N(1), N(2), N(3) plane (Au–Cl(2) off normal by 6.4°; Au–Cl(3), by 3.8°). Both of these observations tend to support bonding interactions between the gold and the axial chlorine atoms.

The EXAFS results are compared to those of the single-crystal structure in Table IV. Agreement in bond length and coordination number is good for the equatorial plane and very poor for the axial Au–Cl bonds.

The question of the strength of the bonding interaction between the gold and the axial chlorine atoms led us to examine the Raman spectra of the title complex both in the solid state and in solution. The Au–Cl stretching vibrations for $K(AuCl_4)$ occur at 326 and 349 cm^{-1}. In accord with that observation, we assign the band at 368 cm^{-1} to the stretch of Au–Cl(equatorial) and that at 258 cm^{-1} to an axial Au–Cl stretch. We observe only one axial stretch for reasons unknown to us; perhaps we are unable to detect the lower frequency stretch due to the high background signal within 250 cm^{-1} of the exciting line. More significantly, the spectrum obtained for the aqueous solution is identical with that of the solid except for a slight shift in energy for the observed Au–Cl stretching frequencies. These bands occur at 255 and 374 cm^{-1} for the solution as compared with 258 and 368 cm^{-1} for the solid.

If the axial chlorine atoms had been replaced by solvent water molecules, the Raman spectrum would reflect the change in these lower energy Au–Cl stretching frequencies. The absence of a significant change in the solution spectrum indicates that the bonds between the gold and the axial chlorine atoms remain intact in an aqueous medium.

In conclusion, two main themes emerge from this study. First, not only are six-coordinate gold(III) molecules to be found in the solid state but also these molecular entities with their long fifth and sixth bonds appear to be stable solution species as well. Second, it seems that EXAFS, while being a valuable tool for determining structural information about short-range interatomic distances, is quite restricted in its ability to elucidate structural information for longer range interactions. For systems that require such knowledge, other techniques may be applied. These include single-crystal X-ray diffraction when crystals can be obtained or the use[25] of wide angle X-ray scattering (WAXS) and differential anomalous scattering (DAS) for amorphous solids and solutions.

Acknowledgment. We thank the NSF for support (Grant PCM 8402651). EXAFS experiments were performed at the SSRL, which is operated by the Department of Energy.

Registry No. $Au(diene)Cl_3$, 99618-00-5.

Supplementary Material Available: Tables A–D, showing F_c and F_o values, hydrogen atomic positional parameters, anisotropic thermal parameters, and root-mean-square displacements for $Au(dien)Cl_3$ (12 pages). Ordering information is given on any current masthead page.

(23) Pauling, L. E. "The Nature of the Chemical Bond", 3rd ed.; Cornell University Press: Ithaca, NY, 1960; p 260.
(24) Duckworth, V. F.; Stephenson, N. C. *Inorg. Chem.* **1969**, *8*, 1661.
(25) Elder, R. C.; Ludwig, K.; Cooper, J. N.; Eidsness, M. K. *J. Am. Chem. Soc.* **1985**, *107*, 5024.